

Development of a novel agitated vessel for gas-induction to improve the gas-liquid mass transfer

G. Chinnasamy^{1*}, S. Kaliannan¹, P. M. Jeganathan²

¹Department of Chemical Engineering, Kongu Engineering College, Perundurai, Erode-638060, Tamilnadu, India

²Department of Food Science and Nutrition, Periyar University, Salem-636011, Tamilnadu, India

Received: February 06, 2019; Revised: February 20, 2020

A novel agitated vessel was developed for improving the gas-liquid mass transfer by a self-inducing mechanism. The effects of aeration time, orifice submergence depth (0.10 - 0.30 m), total gas-free liquid level (0.20 - 0.40 m) and impeller speed on the dissolved oxygen content of water and the volumetric mass transfer coefficient were investigated. The results indicated that the dissolved oxygen content of water increased with increase in aeration time and reached an equilibrium value. It was also noticed that the time required for attaining the equilibrium value of dissolved oxygen content increased with increase in orifice submergence depth and hence with increase in total gas-free liquid level. The volumetric mass transfer coefficient was found to increase with increase in rotational speed of the impeller but decreased with increase in liquid level to tank diameter ratio (H/T) at all the impeller speeds chosen for the present work.

Keywords: air-inducing reactor, critical speed, gas holdup, dissolved oxygen, mass transfer coefficient.

Nomenclature: C – Dissolved oxygen concentration in water at time t , mg/L; C_0 – Initial dissolved oxygen concentration in water, mg/L; C^* – Equilibrium dissolved oxygen concentration in water, mg/L; D – Diameter of the impeller, m; h – Orifice submergence depth, m; H – Total gas-free liquid height, m; ID – Inner diameter, m; k_{La} – Volumetric mass transfer coefficient, min^{-1} ; N – Rotational speed of the impeller, rpm (revolutions per minute); OD – Outer diameter, m; P – Shaft power, kW; P/V – Power consumption per unit volume of the gas-free liquid, W/m^3 ; t – Time, min; T – Tank diameter, m; V – Volume of the gas-free liquid, m^3 ; ε_G – Fractional gas holdup.

INTRODUCTION

Hydrogenation of a variety of substances, ozonolysis, oxidation, alkylation, hydrochlorination and hydrobromination, halogenation, ammonolysis, etc. are industrially important unit processes, which necessitate the complete utilization of the solute gas to a practically possible extent. In a conventional agitated vessel used for gas-liquid operation, the gas is sparged at the bottom of the tank in the form of bubbles and the gas-liquid system is well agitated in order to improve the effective utilization of the gas. But in most of the gas-liquid operations/processes carried out in a conventional agitated vessel, the utilization of gas in a single pass is considerably low due to the low residence time of the gas in the liquid. The utilization of the gas phase in such systems could be improved by external recycling of the unused/unreacted gas, which requires additional energy. Surface aeration is one of the options for internal recycling of the gas in an agitated vessel; but involves some limitations such as high maintenance requirement, inefficient aeration, limited mixing performance, inefficiency at higher liquid depths, etc. Self-inducing type of agitated vessels could provide better contact between gas and liquid at relatively lower power consumption when compared

with surface aerators [1–8]. Moreover, by using self-inducing reactors, the solid particles could be kept in suspension at relatively lower impeller speeds than that required by a surface aerator [9, 10].

The gas-inducing reactors found in the literature have a hollow shaft and a hollow impeller. The acceleration of the fluid caused by the rotation of the impeller leads to a reduction in the static pressure. When the area of the low pressure is connected to the gas space, and the reduction in pressure is higher enough to overcome the resistances in the path of the gas, induction of the gas takes place [9–11]. Apart from the hollow-impeller and hollow-shaft combination for gas-induction, stator-rotor (draft-tube) type of gas-induction is also found in the literature [12, 13]. There have been continuous modifications in the design and fabrication of air-inducing reactors over the past three decades [14]. However, all the air-inducing reactors reported so far in the literature could be classified into any one of the three types, namely, stator-rotor type, hollow-impeller and hollow-shaft type and surface aerator type, respectively. Of the three types of air-inducing reactors, the hollow-impeller and hollow-shaft types were investigated by the majority of the researchers. There are many complications in the design and fabrication of hollow-impeller and hollow-shaft type

* To whom all correspondence should be sent:
E-mail: cgomadurai@gmail.com

of the air-inducing reactors due to their complicated geometry. Moreover, the mechanisms of air-induction reported in the literature necessitate the complete fabrication of an air-inducing impeller system, and cannot convert a conventional agitated vessel into an air-inducing reactor.

In the present study, a novel method was developed for self-induction of air in order to improve the gas-liquid mass transfer performance of a self-inducing agitated vessel. A self-inducing tube set was designed, fabricated and attached to the impeller shaft for converting a conventional agitated vessel into a self-inducing reactor. The gas-liquid mass transfer performance of the newly developed self-inducing reactor was analyzed by taking water as the working fluid and measuring the dissolved oxygen content of water upon induced aeration under various operating conditions.

EXPERIMENTAL

In order to study the performance of the novel air-inducing impeller, a conventional baffled agitated vessel retrofitted with a specially designed air-inducing tube-bundle was fabricated. The schematic diagram of the experimental setup is shown in Fig. 1.

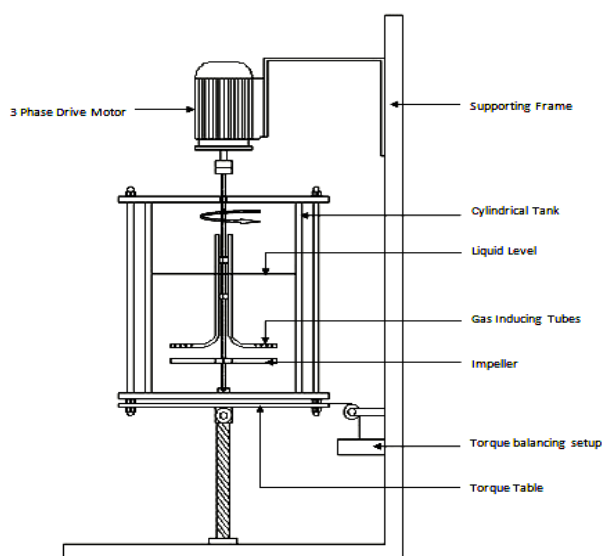


Figure 1. Experimental setup of the gas inducing mechanically agitated contactor.

Agitated vessel

A flat-bottomed cylindrical agitated vessel of 0.455 m inner diameter, 0.012 m wall thickness, and 0.570 m height, made up of acrylic material, was mounted on a torque-table fixed to the floor. Four vertical baffles were fitted to seize the vortex formation and ensure effective mixing of the working fluid. The impeller diameter and the baffle width were 1/3 and 1/10 of the inner diameter of

tank, respectively. The impeller, mounted on a vertical solid shaft, was driven by a 2 hp, 3-phase AC induction motor (Monark, Stark Motors, India). The rotational speed (N) of the impeller was regulated by a speed control drive (Commander SK, Emerson, India) and the power consumed by the motor was measured using two single phase digital wattmeters (Ampere, India). The shaft power (P) was calculated from the counter weight on a load cell which was connected to the torque table. The impeller speed was measured using a digital tachometer (Systems, India). The vessel was covered to avoid surface aeration.

Tube bundle

The tube bundles used for inducing air into the vessel were fabricated using stainless steel tubes (SS306, 10 mm OD, 7 mm ID) bent to 'L' shape (height of vertical section: 345 mm; length of horizontal section: 140 mm) and welded vertically to two hub rings (10 mm ID, 25 mm OD) at an equiangular radial array with the horizontal ends facing outwards. The tube bundle was fabricated using 6 tubes. The tube ends at the horizontal section of the tube bundle were closed and those of the vertical section were left open. There were eight 2-mm orifices arranged in two opposite rows in the horizontal section of each tube in the tube bundle.

The tube bundle was attached to the impeller shaft by means of scrub screws in order to make the tube bundle run along with the impeller shaft. For all experimental runs, the horizontal section of the tube bundle was immersed in the liquid and the tube ends at the vertical section were above the liquid level in the reactor. In addition to the impeller assemblies, the bottom clearance and the submersion depth of the horizontal section of the primary impeller (i.e., the submersion depth of the orifices) were varied by sliding and fixing the hub-rings on to the shaft. The schematic diagrams of the air-inducing tube set and the six-bladed straight-blade turbine are shown in Fig. 2.

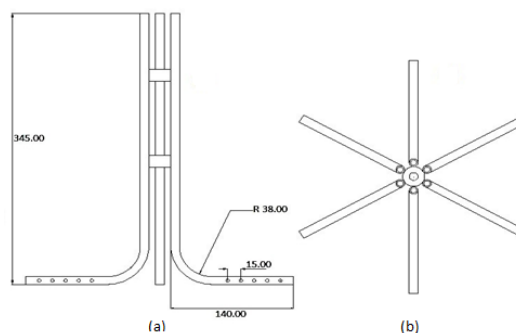


Figure 2. Air-inducing tube bundle (a) front view, (b) top view.

In order to study the performance of the self-inducing agitated vessel for gas-liquid mass transfer, tap water was used as the working fluid and the dissolved oxygen content of water was measured using dissolved oxygen meter (Hanna HI-9142, India). Initially sodium sulphite was gradually added to water to expel the residual dissolved oxygen content from water. The rotational speed of the impeller was maintained at various levels from 3.33 s^{-1} (200 rpm) to 10 s^{-1} (600 rpm) with an increment of 1.67 s^{-1} (100 rpm) using the speed control drive. At each impeller speed maintained, the dissolved oxygen content of the water was recorded against time until the equilibrium dissolved oxygen content

was reached. The total gas-free liquid level in the tank was varied from 20 cm to 40 cm. The impeller speed was measured by a tachometer, the fractional gas holdup was determined by measuring the levels of the working fluids before and after the induction of air [13, 14] and the power consumption was measured using torque table and load cell. The effects of impeller speed, initial gas-free liquid level in the tank and orifice submergence depth on fractional gas holdup, dissolved oxygen content, mass transfer coefficient and power consumption were determined. The details of the initial conditions maintained for the measurement of dissolved oxygen content in water are presented in Table 1.

Table 1. Initial conditions for mass transfer studies by dissolved oxygen measurement.

Impeller speed (rpm)	Tube set clearance (m)	Impeller clearance (m)	Orifice submergence depth (m)	Total liquid level (m)
200	0.10	0.10	0.10	0.20
			0.15	0.25
			0.20	0.30
			0.25	0.35
			0.30	0.40
300	0.10	0.10	0.10	0.20
			0.15	0.25
			0.20	0.30
			0.25	0.35
			0.30	0.40
400	0.10	0.10	0.10	0.20
			0.15	0.25
			0.20	0.30
			0.25	0.35
			0.30	0.40
500	0.10	0.10	0.10	0.20
			0.15	0.25
			0.20	0.30
			0.25	0.35
			0.30	0.40
600	0.10	0.10	0.10	0.20
			0.15	0.25
			0.20	0.30
			0.25	0.35
			0.30	0.40

The volumetric mass transfer coefficient $k_L a$ was determined by:

$$k_L a = \frac{\ln\left(\frac{C^* - C_0}{C^* - C}\right)}{t} \quad (1)$$

where, C^* = equilibrium dissolved oxygen concentration in water, mg/L, C_0 = initial dissolved oxygen concentration in water, mg/L and C = dissolved oxygen concentration in water at time t .

RESULTS AND DISCUSSION

Effect of rotational speed of the impeller on fractional gas holdup in water

The variations of fractional gas holdup in water with variations in rotational speed of the impeller for an air-inducing tube set with 6 tubes along with a six-bladed straight-blade turbine impeller for bottom clearance of 0.10 m for straight blade turbine impeller and 0.10 m for air inducing tube set are presented in Fig. 3. For a given liquid level in the tank, the increase in impeller speed increased the rate of induction of air into the vessel and hence there was a corresponding increase in the fractional gas holdup in the liquid for all five liquid levels, viz., 0.20, 0.25, 0.30, 0.35 and 0.40 m in the vessel. Inclusion of this new type of air-inducing tube bundle to the agitated vessel provides results similar to those observed by previous researchers who used several different methods for the induction of air [15, 17–19].

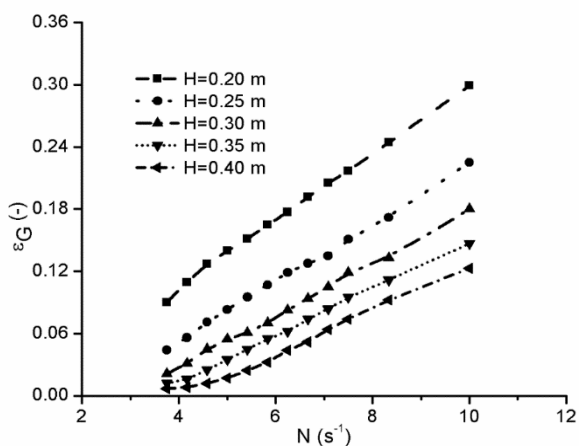


Figure 3. Effect of the rotational speed of the impeller on fractional gas holdup in water for an air-inducing tube set with 6 tubes along with a six-bladed straight-blade turbine impeller for bottom clearance of 0.10 m for a straight-blade turbine impeller and 0.10 m for an air-inducing tube set.

Effect of rotational speed of the impeller on the dissolved oxygen concentration of water

The effect of rotational speed of the impeller on the dissolved oxygen concentration of water for an orifice submergence depth of 0.20 m and a gas-free liquid level of 0.30 m is presented in Fig. 4. It was observed that for a given time of aeration, the dissolved oxygen content of water increased with increase in rotational speed of the impeller until the equilibrium dissolved oxygen concentration was reached. It was also noticed that the time required for attaining the equilibrium value of dissolved oxygen content in water increased with an increase in orifice submergence depth and an increase in total gas-free liquid level. The reason for this effect is that both the rate of air-induction and the fractional gas holdup decrease with an increase in orifice submergence depth. Since the time required for attaining the equilibrium value of the dissolved oxygen content in water is inversely proportional to the rate of air induction and the fractional gas holdup, the time required for attaining the equilibrium decreases with an increase in orifice submergence depth. Moreover, for a given orifice submergence depth the time required for attaining the equilibrium value of the dissolved oxygen content in water is inversely proportional to the rotational speed of the impeller as the rate of air induction and fractional gas holdup increase with an increase in rotational speed of the impeller [20–22]. The gas holdup observed in this study was higher than the gas holdup level reported in the literature [7–9, 22].

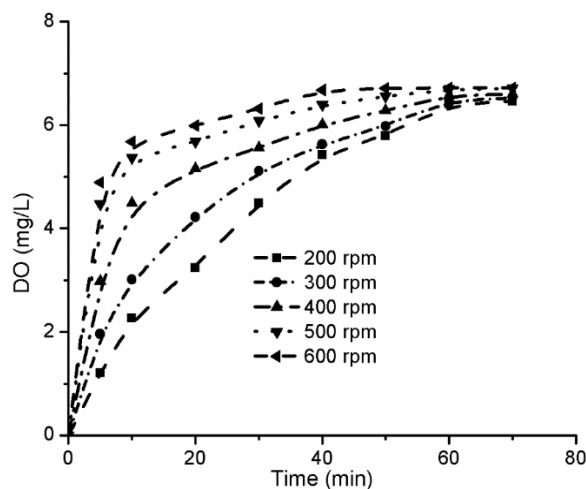


Figure 4. Effect of the rotational speed of the impeller on the dissolved oxygen concentration of water for orifice submergence depth of 0.20 m and gas-free liquid level of 0.30 m for different impeller speeds.

Effect of the rotational speed of the impeller on the volumetric mass transfer coefficient

The variations in volumetric mass transfer coefficient with variations in rotational speed of the impeller are presented in Fig. 5 for orifice submergence depth of 0.25 m and gas-free liquid level of 0.35 m. The volumetric mass transfer coefficient was found to increase with an increase in rotational speed of the impeller for all orifice submergence levels. This behavior was attributed to the fact that the volumetric mass transfer coefficient increases with an increase in the interfacial area between water and the induced air bubbles. Since the increase in rotational speed of the impeller leads to an increase in air induction rate, gas holdup and hence the increase in mass transfer area, the volumetric mass transfer coefficient increases with an increase in rotational speed of the impeller for all orifice submergence depths.

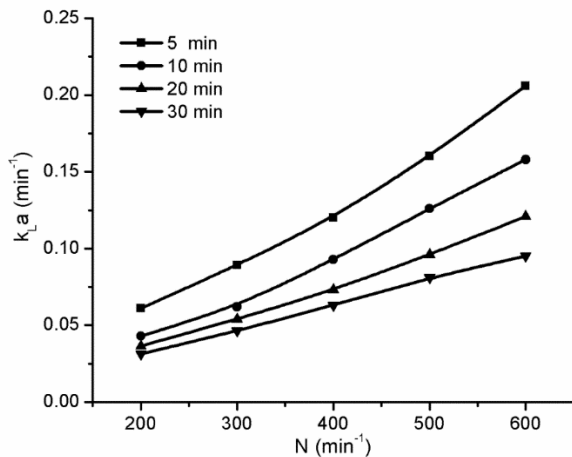


Figure 5. Effect of the rotational speed of the impeller on the volumetric mass transfer coefficient for orifice submergence depth of 0.25 m and gas-free liquid level of 0.35 m.

It was noticed that for a given orifice submergence depth and a given rotational speed of the impeller, the volumetric mass transfer coefficient decreased with an increase in the time of induced aeration [8, 20]. This is due to the fact that the rate of oxygen transfer from the induced air to the water is inversely proportional to the dissolved oxygen concentration in water. Initially the dissolved oxygen content of water is brought to zero by expelling the residual dissolved oxygen content of water by using sodium sulphite, but during the induced aeration of water, the dissolved oxygen concentration of water starts to continuously increase until reaching the equilibrium value. Since the difference between the equilibrium value of dissolved oxygen content of water and the actual

oxygen content of water, which is the driving force for the transfer of oxygen from induced air to the water, decreases continuously during induced aeration, the volumetric mass transfer coefficient decreases with an increase in time of induced aeration.

Effect of liquid level to tank diameter ratio on volumetric mass transfer coefficient

Fig. 6 shows the effect of liquid level to diameter ratio on the volumetric mass transfer coefficient for 30 min of induced aeration time for impeller speeds of 200, 300, 400, 500 and 600 rpm. It was observed that the volumetric mass transfer coefficient decreased with an increase in liquid level to tank diameter ratio (H/T) at all impeller speeds higher than the critical speed. The increase in liquid level to tank diameter ratio indicates an increase in liquid level in the tank. Therefore, when the liquid level in the tank increases, the orifice submergence depth also increases. Since the increase in orifice submergence decreases the rate of air-induction, the fractional gas holdup and hence the mass transfer area, the volumetric mass transfer coefficient decreases with an increase in H/T ratio. It was noticed that for a given H/T ratio and a given time of induced aeration, the volumetric mass transfer coefficient increased with an increase in rotational speed of the impeller. The reason for this effect is that the volumetric mass transfer coefficient increases with an increase in gas holdup and interface mass transfer area between water and induced air which increase due to the increase in rotational speed of the impeller.

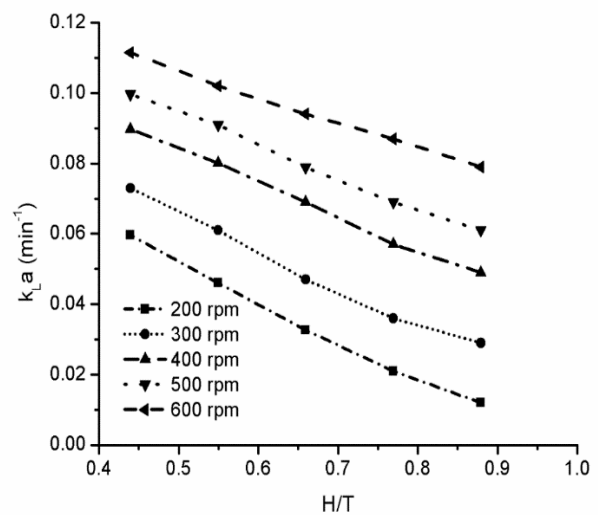


Figure 6. Effect of liquid level to tank diameter ratio on the volumetric mass transfer coefficient for induced aeration time of 30 min.

Effect of power consumption per unit volume of the liquid on the volumetric mass transfer coefficient

The effect of power consumption per unit volume of the liquid on the volumetric mass transfer coefficient is shown in Fig. 7 for orifice submergence depth of 0.20 m and a gas-free liquid level of 0.30 m. It was observed that the volumetric mass transfer coefficient increased with an increase in power consumption per unit volume of the liquid [6, 7]. This behavior of the system was attributed to the fact that the increase in power consumption per unit volume of the liquid indicates an increase in rotational speed of the impeller.

The rate of air-induction, gas holdup and interface mass transfer area increase with the rotational speed of the impeller. Therefore, the volumetric mass transfer coefficient increases with an increase in power consumption per unit volume of the liquid. Moreover, it was noticed that for a given value of power consumption per unit volume of the liquid for a given liquid level, the volumetric mass transfer coefficient decreased with an increase in time of induced aeration.

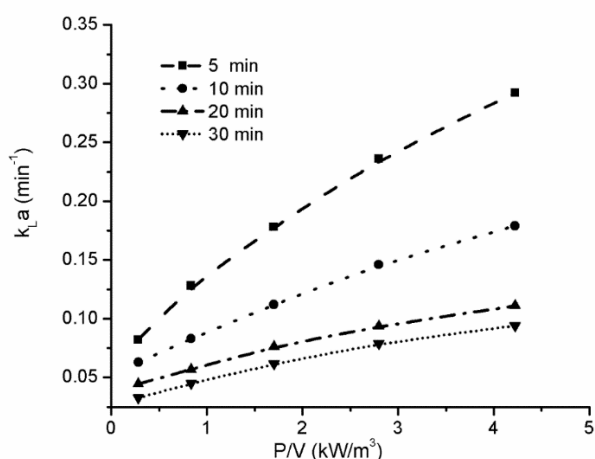


Figure 7. Effect of power consumption per unit volume of the liquid on the volumetric mass transfer coefficient for orifice submergence depth of 0.20 m and gas-free liquid level of 0.30 m.

CONCLUSION

In order to improve the gas-liquid mass transfer in a self-inducing agitated vessel, a novel method was developed and tested. The influence of parameters such as orifice submergence depth (0.10–0.30 m), total gas-free liquid level (0.20–0.40 m) and impeller speed on the dissolved oxygen content of water and the volumetric mass transfer coefficient were studied. The relationship of dissolved content in water *versus* aeration time at various rotational speeds was revealed. When compared with the design and fabrication of the air-inducing reactors

found in the literature, the novel method employed for self-induction of air in this study is the one that requires the simplest modification for converting a conventional agitated vessel into an air-inducing reactor. The analysis of the results indicated that for impeller speeds less than 10 rps, the gas holdup and the volumetric mass transfer coefficient of the novel air-inducing reactor used in the present work are significantly higher than the gas holdup and the volumetric mass transfer coefficient reported in the literature [7–9, 22]. Hence, it is clear that the novel air-inducing reactor developed in this study can be an alternative wherever a higher gas holdup is required for gas-liquid operations/processes.

REFERENCES

1. M. Jafari, J. S. S Mohammadzadeh, *Chem. Eng. J.*, **103**, 1 (2004).
2. S. S. Patil, V. D. Mundale, J. B. Joshi, *Ind. Eng. Chem. Res.*, **44**, 1322 (2005).
3. N. A. Deshmukh, S. S. Patil, J. B. Joshi, *Chem. Eng. Res. Des.*, **84** (A2), 124 (2006).
4. F. Scargiali, R. Russo, F. Grisafi, A. Brucato, *Chem. Eng. Sci.*, **62**, 1376 (2007).
5. Z. Wang, P. Xu, X. Li, S. Wang, Z. Cheng, F. Ju, *Chem. Eng. Process.*, **69**, 63 (2013).
6. J. H. Chen, Y. C. Hsu, Y. F. Chen, C. C. Lin, *Water Res.*, **37**, 2919 (2003).
7. R. B. Kasundra, A. V. Kulkarni, J. B. Joshi, *Ind. Eng. Chem. Res.*, **47**, 2829 (2008).
8. S. Poncin, C. Nguyen, N. Midoux, J. Breyse, *Chem. Eng. Sci.*, **57**, 3299 (2002).
9. J. B. Joshi, M. M. Sharma, *Can. J. Chem. Eng.*, **55**, 683 (1977).
10. S.B. Sawant, J.B. Joshi, *Chem. Eng. J.*, **18**, 87 (1979).
11. A. D. Raidoo, K. S. M. S. R. Rao, S. B. Sawant, J. B. Joshi, *Chem. Eng. Commun.*, **54**, 241 (1987).
12. D. A. White, J. U. De Villiers, *Chem. Eng. J.*, **14**, 113 (1977).
13. M. Major-Godlewska, D. Radecki, *Pol. J. Chem. Technol.*, **20** (1), 7 (2018).
14. V. Sivakumar, K. Senthilkumar, T. Kannadasan, *Pol. J. Chem. Technol.*, **12** (4), 64 (2010).
15. F. Ju, Z. M Cheng, J. H. Chen, X. H. Chu, (2009). *Chem. Eng. Res. Des.*, **87**, 1069 (2009).
16. C. Gomadurai, K. Saravanan, E. Abraham, N. Deepa, *N. Korean J. Chem. Eng.*, **33** (4), 1181 (2016).
17. R. Fakuda, M. Tokumura, H. T. Zand, Y. Kawase, *Chem. Eng. Res. Des.*, **87**, 452 (2009).
18. A. Kielbus-Rapala, J. Karcz, *Chemical Papers*, **64** (2), 154 (2010).
19. F. Yang, S. Zhou, X. An, *Chinese J. Chem. Eng.*, **23**, 1746 (2015).
20. K. Souidi, A. Mardaru, M. Roudet, A. Marcati, D. D. Valle, G. Djelveh, *Chem. Eng. Sci.*, **74**, 287 (2012).
21. D. H. Song, H. D. Kim, K. C. Kim, K. C., *Opt. Laser Eng.*, **50**, 74 (2012).
22. R. Achouri, S. B. Hamza, H. Dhaouadi, H. Mhiri, P. Bournot, *Energ. Convers. Manage.*, **71**, 69 (2013).